crystals

MDPI

Communication

Metal Ion Microwave-Assisted Depolymerization of Poly(Ethylene Terephthalate): A Zinc Salts-Based Deep Eutectic Solvent as Case Study

Cosimo Ricci [1,†], Lorenzo Gontrani [1,†], Elvira Maria Bauer [2], Giorgia Ciufolini [1], Angelo Lembo [1], Lorenzo Casoli [1] and Marilena Carbone [1,*]

[1] Startnetics, Department of Chemical Science and Technologies, University of Rome Tor Vergata, Via della Ricerca Scientifica 1, 00133 Rome, Italy; cosimo.ricci@uniroma2.it (C.R.); lorenzo.gontrani@uniroma2.it (L.G.); giorgia.ciufolini@uniroma2.it (G.C.); angelo.lembo@uniroma2.it (A.L.)
[2] Institute of Structure of Matter-Italian National Research Council (ISM-CNR), Via Salaria Km 29.3, 00015 Monterotondo, Italy; elvira.bauer@ism.cnr.it
* Correspondence: carbone@uniroma2.it
† These authors contributed equally to this work.

Abstract: In this study, a new and very quick method to depolymerize PET plastics is reported. The depolymerization experiments were conducted using a type-IV deep eutectic solvent containing $ZnCl_2$ and urea, and a microwave oven as reactor. Different combinations of power and reaction times were employed while keeping the total energy constant. Successful conversions were obtained carrying out the process at 180 W for 2 min and 360 W for 1 min, whereas at higher powers and shorter times, an inclusion likely occurs of some solvent into the structure of the recovered PET flakes, as suggested by the porosity of the flakes, imaged by SEM microscopy. The flakes increase their crystalline character during the treatment, as indicated by the appearance of narrow diffraction peaks in the XRD patterns, at variance with the broad signals observed in the case of the pristine amorphous polymer. The NMR analysis of the supernatant liquid above the partially solubilized PET shows the presence of terephthalic acid peaks. The infrared spectra of the solid powder achieved upon the acidic treatment of the extract reveal the presence of C=O stretching peaks and the absence of typical CH_2 wagging absorptions that satisfactorily comply with the presence of terephthalic acid.

Keywords: PET; DES; hydrolysis; microwave; plastic recycling; dissolution; green methods; terephthalate; zinc; urea

Citation: Ricci, C.; Gontrani, L.; Bauer, E.M.; Ciufolini, G.; Lembo, A.; Casoli, L.; Carbone, M. Metal Ion Microwave-Assisted Depolymerization of Poly(Ethylene Terephthalate): A Zinc Salts-Based Deep Eutectic Solvent as Case Study. *Crystals* **2024**, *14*, 567. https://doi.org/10.3390/cryst14060567

Academic Editor: Ruikang Tang

Received: 11 April 2024
Revised: 29 April 2024
Accepted: 14 June 2024
Published: 19 June 2024

1. Introduction

Plastic is one of the most widely used materials in the world because it is affordable, lightweight, and extremely durable, but proper end-of-life management is essential in order to meet growing environmental concerns [1–3]. For this reason, processing plastic trash requires high-quality recycling, thus lessening the need for raw materials, the energy used during processing, and the amount of plastic waste that ends up in landfills. Among all plastics, PET (polyethylene terephthalate) displays several properties that make it suitable for numberless applications. It is used in packaging, due to its ability to keep food, since it is a fairly inert polymer, with little or no interaction with the food content. It is very resistant, lightweight, and has the ability to build an oxygen and water barrier, making it ideal for use in beverage bottles. Additionally, it may be used to make translucent bottles, something that polypropylene (PP) or polyethylene (PE) cannot accomplish [4,5]. As a consequence of the large quantity produced and of the increased public awareness, every day more efficient recycling processes are being actively developed [6–9], thus becoming simpler and more affordable thanks to ongoing technological advancements, and PET recycling rates are rising and becoming more significant, as indicated by a number of variables [10]. A major

push comes from regulatory agencies, which recently issued laws providing directives to limit the use of raw materials in favor of recycled ones. For instance, the European Union has implemented new rules mandating that, by 2025 and 2030, beverage bottles must have 25% and 30% of recycled material, respectively [11]. Regarding the details of PET recycling, five types of processes have been described, classified as zero, first, second, third, and fourth-order recycling [12]. In the first type of procedures, for instance, bottles are refilled or remodeled, profiting from the material thermoplasticity. In the second case, unsatisfactory/non-compliant objects are re-used as raw materials and mixed with some fresh one. The third option (second order) refers to physical/mechanical processes, wherein the collected material is washed, pelletized/grinded, and finally fused and extruded. Third-order recycling collects all the chemical transformation methods, whereas in the last possibility the plastic is burnt to produce energy. Among all the possibilities, probably the majority of treatments performed so far include physical manipulations. For instance, PET scraps recovered from water bottles are commonly melted down and turned into fibers to make carpets, pile cardigans, and fiberfill, thus entering the so-called B2F (bottle to fibers) pathway instead of producing new bottles [13,14]. Among the classes defined above, chemical recycling grants maximal versatility, because its goal is to partially or completely disassemble the waste plastic into its original monomers or a recycled "pre-polymer"; the recovered moieties can be finally used as such or mixed with other virgin material [15]. Additionally, two main advantages can be found in this method, namely the possibility of treating wastes that are extremely polluted and heterogeneous and cannot be mechanically recycled, such as multilayered food containers or mixed fiber fabrics [16,17]. Second, it permits the production of monomers that are exactly identical to those derived from fossil feedstocks, even when beginning with polluted and low-quality wastes. These monomers may then be utilized to manufacture high-quality polymers. In consequence of such important features, there has been an increasing focus on the chemical breakdown and recycling of PET materials in recent years, and the primary sought-for monomers are terephthalic acid (TA, Figure 1-left panel) and ethylene glycol (EG). Such compounds can undergo a polycondensation process that ultimately yields the polymer, which is then turned into the final objects. The most critical material of the two components is TA, which is principally produced by the oxidation of poly-xylene (PX) in an acetic acid solution [18], typically using $Co(CH_3COO)_2$ as catalyst [12]. PX manufacturing is a complex process, and TA production has comparatively high costs; it is therefore extremely important to recover TA from waste PET materials. Among the techniques employed to perform such a task, alcoholysis, aminolysis, hydrolysis, and other processes [19–21] have been considered. Glycolysis, which uses EG as a solvent, is one of the most common alcoholysis techniques; in order to speed up the degradation process, deep eutectic solvents (DESs) [22] and a variety of ionic liquids (ILs) were employed as catalysts [23]. For instance, Zhang's group realized the glycolysis of PET using first-row transition metal-containing ionic liquids as catalysts [24]; the glycolysis of PET was also carried out using urea/$ZnCl_2$ DESs as catalysts [25], whereas the ionic liquid [Bmim][OAc] was used to degrade PET in glycol [26]. When glycolysis processes are operated, bis(2-hydroxyethyl) terephthalate (BHET, Figure 1-right panel) is the principal breakdown product of PET materials.

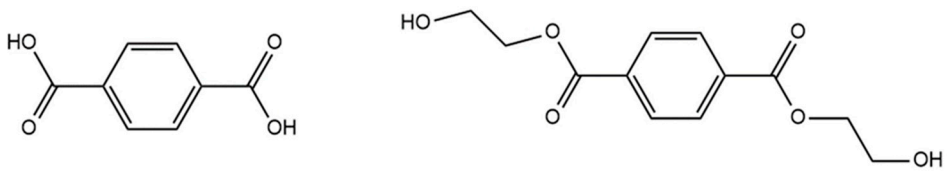

Figure 1. Chemical structure of TA (**left**) and BHET (**right**).

During the glycolysis, additional catalysts were also employed, such as zinc acetate, sodium carbonate, solid acid (SO_4^{2-}/Co_3O_4) [27], metal oxides, and polyoxometalate (POMs) like $K_6SiW_{11}MO_{39}$, which was utilized to complete PET glycolysis in autoclave

at 185 °C [28] or dual-active site tungsten-based sandwich POMs [29]. Moreover, BHET was produced by both supercritical and subcritical glycolysis [30]. Still in the field of supercritical fluids, supercritical methanolysis [31] is another significant alcoholysis technique [32], which yields dimethyl terephthalate, whereas if supercritical ethanol is used in conjunction with [Bmim][BF_4] IL as a catalyst, the main product of PET decomposition is dimethyl terephthalate, which can be successfully recovered [33]. Regarding PET aminolysis, Zhen Leng's group carried out the reaction in ethanolamine, with the resultant product being used to produce modified asphalt [31]. In a different study by the same author, the bituminous mixture performance was enhanced by using the PET aminolysis product obtained in triethylenetetramine [34]. The molecules that were left over after degradation were amides, and more reaction was required to produce monomers. In another study, alkyl amines, such as ethanolamine, were used as solvents in the breakdown of PET [35], whereas aminolysis using bicyclic guanidine derivative 1,5,7-triazabicyclo[4.4.0]dec-5-ene (TBD) as active ingredient was successfully employed by Fukushima's group [36] to recover BHET from PET flakes at 78% yield. Turning to hydrolysis, it can be carried out in aqueous solution employing a metal salt or solid acid as a catalyst. For instance, PET was solubilized in hot compressed water containing $Zn(CH_3COO)_2$ [37]; the reaction products were TA and EG in this case. In Wang et al.'s [25] research, a highly concentrated aqueous $ZnCl_2$ solution demonstrated excellent catalytic properties for the breakdown of synthetic polymer materials. For example, the authors report that polyurethane C-N and C-O bonds could be broken selectively in a hydrothermal reaction at 180 °C using a $ZnCl_2/H_2O$ solution. In this regard, it has been known for some time that transition metal salts, in particular oxides, possess sublime properties in this field as well as in other technological domains [38–47]. In addition to alcoholysis, hydrolysis, and ammonolysis, various non-conventional procedures were used to recycle PET materials. The dissolution was achieved, for instance, employing Ideonella Sakaiensis 201-F6 bacterial strains [48], which secrete a hydrolase enzyme [49], responsible for the degradation. Using waste PET as the starting material, Tuan Amran Tuan Abdullah's group obtained hydrogen by steam reforming, which was aided by an Al_2O_3/La_2O_3 catalyst supported on Ni/Pd [50]. Also, the most recently developed solvating systems, ionic liquids (ILs) [51] and DESs, are finding applications in PET recycling directly as reactants/reaction media, besides the already cited role as catalysts [33]. A few ILs show good solvating capabilities for PET and BHET [52], though the separation of BHET proved to be challenging and ILs are more costly compared to $ZnCl_2$. Rather interesting results were recently achieved using type-IV DES (Lewis acid DES, LADES), containing basic hydrogen bond donors (HBDs) as well as acidic ones. To the first group belongs the study by Liu and coworkers [52], who report on the successful synergistic effect of Zn^{2+} (Lewis acid) and dimethyl urea (DMU, Lewis base) in the glycolytic degradation of PET with zinc acetate:DMU at various ratios, which achieved a 100% conversion and very high (82%) BHET yield. DESs based on hexa-hydrated $FeCl_3$ and acidic HBD were taken into account by Rollo et al. [53], who found that the best HBDs were sulphonic acids, which were able to quantitatively transform PET into TA at 100 °C, with high recovery percentages. In a very recent work by the same group [54], the same iron salt was coupled to acetic acid in a proof-of-principle microwave-based experiment where the yield of TA monomer was raised from 4% to 54% by a sodium hydroxide post-treatment. Rather successful results were obtained also with the aid of less conventional reaction schemes that encompass depolymerization steps through microwave-assisted reactors, as reported in several works by Azeem and coworkers, who were able to degrade PET to TA, monohydroxyethyl terephthalate (MHET) and BHET using a series of sequential depolymerization processes in EG—choline chloride-(thio)urea DESs mixtures (glycolysis) followed by a treatment with sodium carbonate in EG (hydrolysis) [55]. Considering all the varied reactions discussed so far, it appears that either basic or acidic media can be chosen to drive the degradation, and that both hydrolytic and glycolytic pathways can be followed. The presence of a metal cation as catalytic agent can be very helpful, as it can lead to additional coordination interactions that synergically reinforce the hydrogen

bond ones provided by the DESs [56]. Based on these premises, we decided to combine the various approaches and investigate the use of different microwave-assisted reaction protocols employing one type-IV DES—also identified as LADES (Lewis Acid DES) [57], namely $ZnCl_2$:urea 1:3.5, one of the $ZnCl_2$:HBD eutectic mixtures, first proposed by Abbott in 2007 [58] and which features a melting point of 252 K. The mixture found applications, among others, in the synthesis of zinc oxychloride nanoparticles [59]. A summary of the procedures described is reported in Figure 2. The experimental setup, i.e., microwaves power and reaction time, keeping the total power constant, were thoroughly explored to optimize PET dissolution and monomer recovery, a comprehensive analysis of the structure of intermediates and final products was carried out using spectroscopic (ATR-FT-IR, UV–VIS, ^{1}H NMR), diffraction (XRD) as well as microscopy (SEM) techniques.

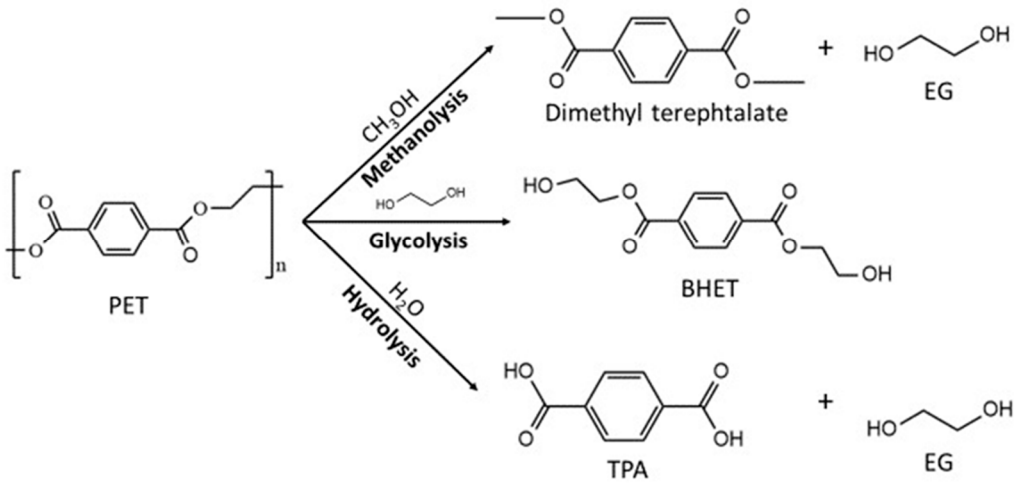

Figure 2. Most common PET dissolution pathways with corresponding products.

2. Materials and Methods

2.1. DES and PET Flakes Preparation

$ZnCl_2$ and urea, $CO(NH_2)_2$, were purchased from Carlo Erba reagents and were used without further purification. DES prepared by mixing $ZnCl_2$ and urea in molar ratio 1:3.5 was named "ZnUD". More in detail, 13.63 g of $ZnCl_2$ and 21 g of urea were placed in a in a 50 mL round bottom flask. The two powders were first blended with a vortex mixer for 1 min, and then a magnetic stirring bar was inserted in the flask, which was placed in an 80 °C oil bath under stirring for 1 h until a clear liquid was obtained. PET flakes were obtained by cutting a transparent PET commercial piece of packaging into 1 mm chips, which were subsequently washed with water and ethanol and finally dried.

2.2. Microwave Treatments

Regarding microwave treatment, 3 g of ZnUD and 100 mg of PET flakes were deposited in a glass vial (Figure 3a) that was placed in the center of the rotating plate of a commercial microwave oven and treated with MW radiation according to different time/power combinations, as shown in Table 1. All the combinations chosen to treat the samples share the same total energy (24 KJ).

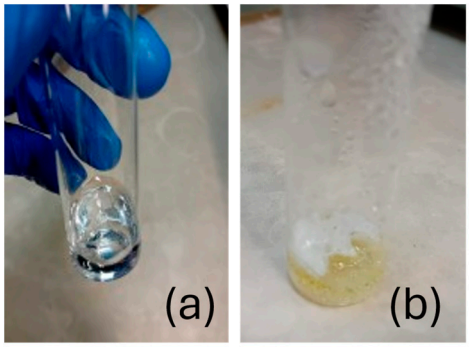

Figure 3. PET flakes immersed in ZnUD (**a**) before and (**b**) after MW treatments.

Table 1. Microwave power and times for the treatments.

Power (W)	Processing Time (mm:ss)
800	00:30
600	00:40
360	01:10
180	02:10

After microwave treatment, the DES forms a light-yellow glass, which was dissolved in 10 mL of a 6% v/v acetic acid solution. The remaining flakes were melted together and easily separated. The PET conversion yield was calculated as follows:

$$\frac{Starting\ PET\ weight - Recovered\ flakes\ weight}{Starting\ PET\ weight} \quad (1)$$

After the acetic acid wash, the DES glass turned into a white powder that was set aside for further investigation.

2.3. Equipment and Methods

Infrared spectra of the flakes and powders were recorded with a Shimadzu Prestige-21 FT-IR instrument (Shimadzu, Kyoto (Japan)), equipped with an attenuated total reflectance (ATR) diamond crystal (Specac Golden Gate), with a resolution of 4 cm^{-1}.

Recovered PET flakes were crushed, and the resulting crystalline powder was analyzed by XRD diffraction, with an X'Pert pro X-ray diffractometer by Philips (Amsterdam, The Netherlands) operated with Cu K_α radiation (λ = 1.54 Å). The spectra were acquired in the 5–90 2θ range, in steps of 0.02 degrees each, with a total counting time of 10 s per point.

The surface morphology of the recovered PET flakes after DES treatment was determined with a SUPRA TM 35 FE-SEM (Field Emission Scanning Electron Microscope), Carl Zeiss SMT, Oberkochen (Germany), operating at voltages between 1.5 and 7 KV.

NMR spectra were collected using a Bruker Avance 700 MHz (^{1}H) instrumentation. The spectra were acquired at 40 °C, using the zg sequence, with a spectral window of 15.9 ppm, 8 scans and 4 dummy scans, using 3 s of acquisition time and 2 s of relaxation delay. A sealed glass capillary filled with deuterated acetonitrile was inserted concentrically into a 5 mm diameter standard NMR sample tube to be used as an external reference signal for the frequency field lock of the instrument. The use of a concentric capillary was necessary to avoid the addition of compounds that could alter the DES system. The capillary was built in-house, from a Pasteur pipette, filled with deuterated acetonitrile, and sealed. To ensure field homogeneity, special attention was given to the stability of the capillary within the NMR tube. For a qualitative measurement, the peak of the residual undeuterated acetonitrile in the spectrum was used as a reference to compare the position of the signals of interest in the spectrum.

3. Results and Discussion

The coveted enhancement in PET depolymerization efficacy by $ZnCl_2$ /urea 1/3.5 DES was explored by the treatments described in Table 1.

The microwave-assisted procedure allows for an overall faster treatment compared to traditional heating, although it still requires the presence of catalysts. Preliminary measurements showed that DES turned into a glass during any treatment that employed an energy larger than 24 J; therefore, such value was fixed as upper energy limit in each treatment performed. More specifically, in the microwave at our disposal, such total energy value can be achieved by combining four different power settings with suitable treatment time, as described in Table 1. In the most powerful setting (800 W for 30 s), a comparatively higher local temperature is achieved for a short time, whereas in all the other experiments a gradual decrease in local temperature along the series 600–360–180 W is realized, thus requiring proportionally longer treatment times to maintain the total energy supplied.

3.1. PET Flakes Weight

During the treatment of PET with liquid ZnUD DES under microwave irradiation, an evident physical change took place, since the originally transparent flakes melted together into a white solid, while the DES became a transparent glass-like amorphous aggregate. Subsequently, the DES glass was solubilized with a 6% acetic acid solution, which ultimately led to its conversion into a white powder. At this point, residual PET flakes could be easily separated, rinsed, air-dried, and weighted, and the conversion yield, reported in Figure 4, could be calculated according to Equation (1). It can be seen that PET was consumed in the 360 W and 180 W treatments, whereas a negative yield was obtained in the 800 W and 600 W treatments. A total of three replicas of the experiment were performed to verify the repeatability.

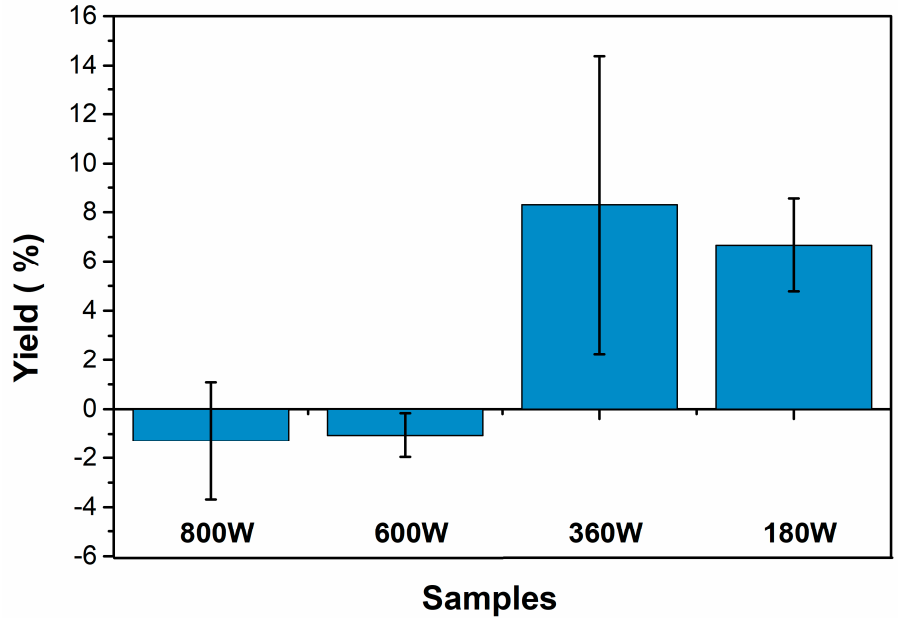

Figure 4. PET conversion yield after microwave treatment at different powers. The mean values and standard deviations are reported.

The negative yield may indicate inclusive and aggregative processes, also considering that PET is capable of gathering solvents, leading to a concomitant swelling. This issue is even more evident for the highest powers, with the 800 W/30 s treatment scoring the most negative yield (−3.7%).

In order to obtain an insight into the process occurring at the molecular level, the recovered flakes were then analyzed by XRD, IR, NMR, and SEM, focusing in particular on

the structural modifications that occurred due to the treatment, with respect to the pristine material.

3.2. XRD

The recovered PET fragments were finely grinded after drying, and the powders were investigated with X-ray diffraction. A highly eye-catching feature of the diffraction patterns (Figure 5) is the marked increase in intensity of the signals observed in the 15–35 2θ range, compared to the pristine polymer, which can be noticed for the samples treated at low power and for a longer time (180 W and 360 W, red and blue curves, respectively), compared to the 600 W and 800 W samples (olive green and magenta, respectively) that show a relative lower degree of crystallinity. Notably, the three tallest peaks identified in our measurements, falling at 17, 23.5, and 26 degrees, comply nicely with the crystalline phase patterns reported in [60], which correspond to reflections originated by 100, $\bar{1}10$, and 010 crystallographic planes and are evidenced as orange ticks in Figure 5. Interestingly, the starting material (green curve) is largely amorphous, while samples processed at 180 W and 360 W develop the well-defined peaks of the crystalline form of PET [60]. A rough estimate of the crystallite size was performed after removal of the amorphous background by using the Scherrer relation outlined below [61,62]:

$$\sigma = \frac{K\lambda}{\beta \cos \theta} \quad (2)$$

which links the average size σ to the radiation wavelength λ, to the scattering angle θ, and to the half of the maximum intensity (FWMH), noted as β. The calculation suggests that, in both 180 W and 360 W samples, the domain size falls in the 5–10 nm range. These results are in compliance with a former study by Guo et al., who treated a water dispersion of PET powder at 200 °C for 2 h [63]. Differently from that study, though, in the present investigation the process was much faster (2:10 min at 180 W), suggesting a possible catalytic role of the DES medium.

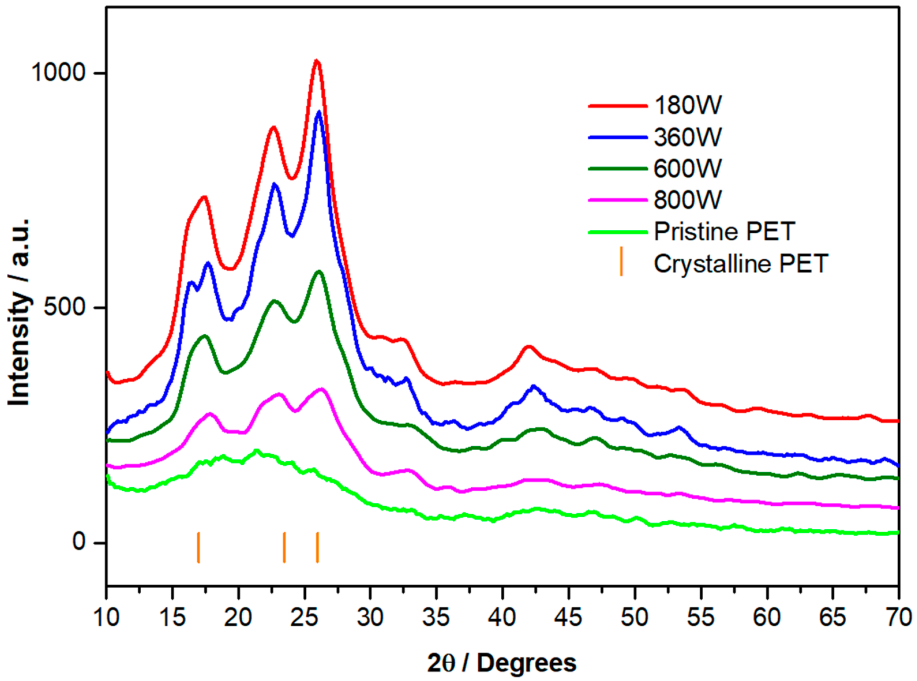

Figure 5. XRD pattern of PET flakes in pristine form and after microwave treatment in the 10–60 2 theta range. Light green: original PET flakes, light blue: 180 W, dark blue: 360 W, dark green: 600 W, magenta: 800 W. The plots have been shifted to improve readability. The three main references of crystalline PET from [60] are reported as orange ticks to guide the eye.

A possible explanation of the counterintuitive increase in crystallinity with the lowest power/temperature settings may be traced to a confined crystallization phenomenon. It has been shown, in fact, that polymer systems can undergo a change from isotropic morphologies to more ordered arrangements whenever the starting melts are confined in space, stimulating the formation of lamellar crystal systems [64]. A similar space confinement phenomenon can be envisaged for the DES mixtures employed in the present study. Actually, it was shown by neutron diffraction and molecular simulation studies that the DES mixture reline (choline chloride:urea 1:2 system) is constituted of a layered sandwich structure wherein chloride anions are confined between urea molecules by hydrogen bonds [65]. In line with this, some of us have recently demonstrated that urea-based DESs exert a marked templating effect in the (co)precipitation of nanoparticles, which inherit the urea planar structure and arrange in a nano-platelet fashion [59]. The large micro/mesoscopical order of DES environment is likely progressively diminished by thermal motions when the temperature is rapidly raised at the highest MW powers employed, whereas it can withstand the heating at lower powers and allow for a sustained crystallization.

3.3. IR Spectroscopy Study

The PET IR spectra of pristine and treated samples are reported in Figure 6a,b. The absorption bands observed in the pristine PET IR spectrum are reported in Table 2. Among the strongest absorption peaks, a very evident signal is found at around 1712 cm^{-1}, which can be assigned to the stretching vibration of an ester C=O moiety, while in the region 1320–1420, a strong absorption mainly ascribable to C=C bonds combined to =C-H bending is found at 1408 cm^{-1}, followed by a pair of medium-strong signals found at 1370 and 1338 cm^{-1}, which are originated by CH_2 wagging (bending) normal modes.

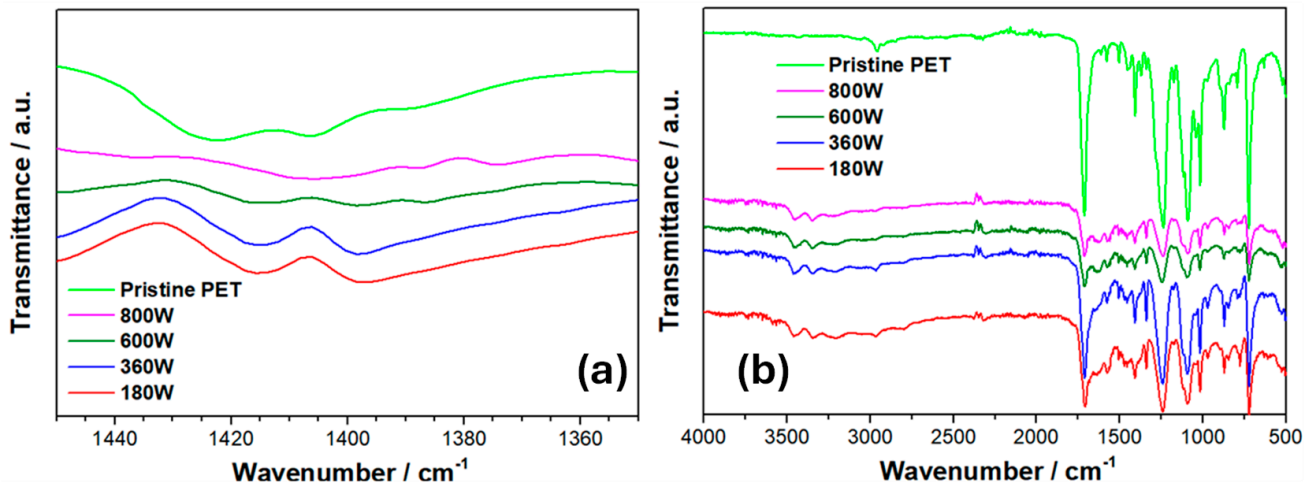

Figure 6. ATR–FTIR IR spectra of a pristine PET flake and of recovered PET flakes after the microwave treatment at different powers shown as (**a**) full spectra and (**b**) in the 400–4000 cm^{-1} range. Green: pristine flakes, red: 180 W, blue: 360 W, olive: 600 W, magenta: 800 W.

Table 2. FTIR peak assignment of pristine PET.

Observed Signal (cm^{-1})	Assignment
2956 ms	CH_2 methylene stretching
2018 vw	CH_2 methylene stretching
2048 vw	CH_2 methylene stretching
1712 vs	C=O carbonyl stretching (ester)
1614 w	C=C ring stretching + =C-H ring in plane bending
1577 mw	C=C ring stretching
1504 mw	=C-H ring in plane bending + C=C ring stretching
1452 m	CH_2 methylene bending + O-CH bending
1408 s	C=C ring stretching + =C-H ring in plane bending
1370 w	CH_2 wagging
1338 w	CH_2 wagging
1267 shoulder	C-O stretching carbonyl + =C-C ring ester stretching + C=O in plane bending
1238 s	
1172 w	=C-H ring in plane bending + C=C ring stretching
	C-O stretching carbonyl + C=C-C ring bending + C=O in plane bending + O-CH_2 stretching
1116 s	C=C ring stretching + C-O carbonyl stretching
1090 s	C-O stretching carbonyl + C-C glycol stretching + C-C-O glycol bending + C-O-C bending
1041 m	C=C-C ring stretching + C=C ring stretching + =C-H ring in plane bending
B 972 w	-O-CH stretching + C-O-CH_2 stretching
875 m	=C-H ring out of plane bending + =C-C ring ester out of plane bending + C=O out of plane bending + ring torsion
843 w	CH_2 rocking
792 mw	-C=O out of plane bending + ring torsion + =C-C ring ester out of plane bending
723 s	=C-H ring out of plane bending + -C=O out of plane bending
632 vw	C=C-C ring bending + =C-C=O ring ester bending
497 m	=C-C=O ring ester stretching + C=O in plane bending

Further on, two distinctive signals fall around 1100 cm^{-1} (1116 and 1090), whose origin can be traced back to C-O single bond stretching, mixed either with C=C ring stretching (1116 cm^{-1}) or with C-C glycol stretching, C-C-O glycol bending and C-O-C bending in the lower wavenumber band (1090 cm^{-1}).

The observed FTIR peaks of pristine PET reported above (Table 2) were assigned according to reference [66]. The post-commercial PET spectra show all the peaks reported in the cited paper without any significant shift in the position, thereby confirming that the pristine PET sample studied was endowed with high purity. Additionally, the recovered flakes mainly retain the original PET infrared absorption pattern, but some new features arise, and others decrease in intensity. In particular, some peaks that may be attributed to vibrations of DES moieties encapsulated into the PET structure appear in the OH/NH stretching region (3250–3500 cm^{-1}), while in the fingerprint region of the spectrum some signals increase their transmittance. It is noteworthy that, in the 1300–1450 cm^{-1} segment, reported in Figure 6, absorption peaks falling at 1340 cm^{-1} and 1370 cm^{-1}, which can be traced back to the wagging normal mode of the polymer glycol moiety in the trans and cis conformations, respectively, undergo relevant changes. In the 180 W and 360 W samples, the former peak gains intensity, while the latter almost disappears, with respect to untreated PET (dark and light blue lines, respectively), suggesting a conversion between the *cis* and

trans conformers of the polymer. This behavior has been attributed to a significant decrease in the amorphous phase by Chen et al. [67]. This issue complies nicely with the confined crystallization previously hypothesized.

3.4. SEM Study of Recovered Flakes

A SEM microscopy study was performed on the pristine PET and on the flakes recovered after the DES treatment. According to the images reported in Figure 7, pristine PET appears completely amorphous with no discernible features, while noteworthy features can be pointed out in 180 W (Figure 7b) and 360 W flakes (Figure 7c).

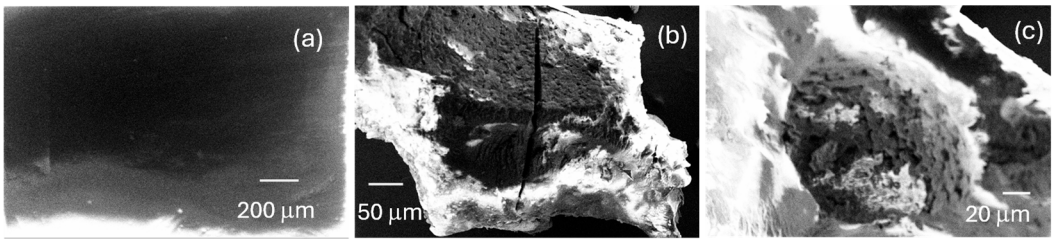

Figure 7. FE–SEM image of a (**a**) pristine PET flake and PET flakes recovered after microwave treatment with ZnUD at (**b**) 180 W and (**c**) 360 W.

The former ones show a rather rough surface and stress fractures, indicating an increase in crystallinity compared to the starting fragments, while the 360 W sample shows a more porous structure with an increased roughness. The observed increase in porosity with treatment power can be considered as the main cause of the negative yield in the reaction conducted at high power (600 and 800 W). Under those conditions, DES fragments may be absorbed by PET flakes, resulting in the apparent negative yield observed (see Figure 4).

3.5. NMR

To identify the product of the reaction that consumes PET inside ZnUD DESs, a series of NMR experiments were carried out and reported in Figure 8.

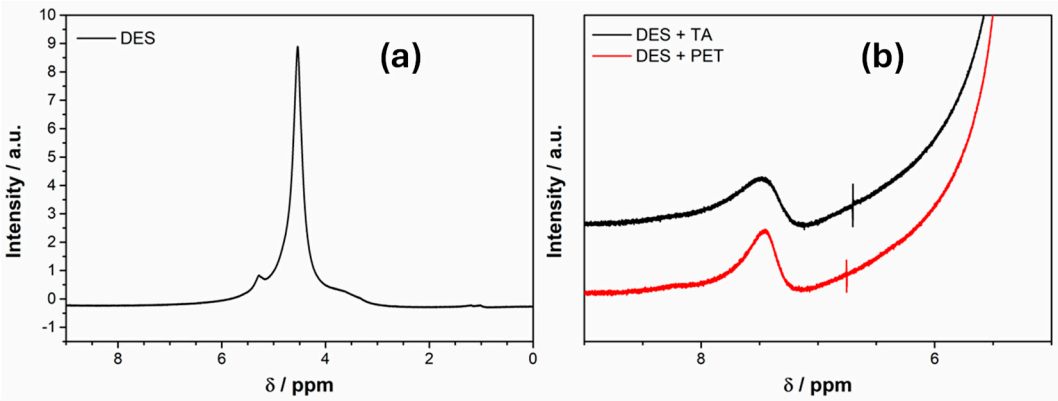

Figure 8. ^{1}H−NMR spectra of (**a**) ZnUD DES, and (**b**) ZnUD DES + TA and ZnUD DES after PET treatment at 180 W for 1 min.

In the first experiment, the DES sample was introduced in the NMR tube, along with a sealed glass capillary filled with deuterated acetonitrile used as an external standard for the instrument lock and kept at 40 °C to ensure fluidity. The spectrum shows only the large urea signal at 4.5 ppm (Figure 8a). To assess the presence of TA as a reaction product, the ^{1}H NMR spectrum of a saturated solution of TA in DES was measured afterwards, maintaining the same procedure, which revealed the TA peak at 7.4 ppm. Finally, 100 mg of PET was treated in 3 g of DES in a microwave at 180 W for one minute. The DES remained

liquid in such conditions, and the PET flakes were easily removed. The solution was then centrifuged, and its NMR spectrum was measured using again deuterated acetonitrile as a standard. Notably, the resulting spectrum of DES + PET shows the same 7.4 ppm peak as the DES + TA solution, thus indicating the presence of TA monomers in the supernatant liquid and suggesting a hydrolysis depolymerization reaction of PET (Figure 8b). Yet, it should be noted at this time that the possible presence of terephthalamide, product of an aminolysis pathway, cannot be completely ruled out, since its peak position is, typically, rather close to that of TA. The latter process would be due to the ammonia molecules that are present in non-negligible concentration in the DES, owing to the partial hydrolysis of urea induced by the presence of absorbed humidity, and also decomposition processes at higher temperatures [68] possibly occurring during microwave treatment.

Moving on to the powder recovered after microwave-assisted treatments in DESs, and ensuing acid recovery, IR spectra were taken and reported in Figure 9 with the reference spectra of terephthalic acid and PET; the observed peaks are assigned in Table 3. The sample peaks are intermingled with the underlying signal coming from the DES matrix. It is interesting to notice that the carbonyl peak of the samples is shifted at lower wavenumbers (1692 and 1678 cm^{-1} for 180 W and 360 W, respectively) compared to pristine PET (1712 cm^{-1}), in which the carbonyl group is part of an ester but is higher than the absorption frequency of TA carbonyl stretching (1671 cm^{-1}). This could be due to the convolution of acid and ester C=O bands in the samples, suggesting the presence of oligomers in which both types of motifs are present [69]. In the region between 1450 and 1300 cm^{-1}, it is possible to notice the almost complete disappearance of the 1340 and 1370 cm^{-1} CH_2 wagging bands related to the ethylene glycol moiety, while the ring stretching band of the TA and PET is still present, albeit at a lower wavenumber compared to TA (1423 and 1405 cm^{-1} for TA, 1415 and 1397 cm^{-1} for the 180 W and 360 W samples).

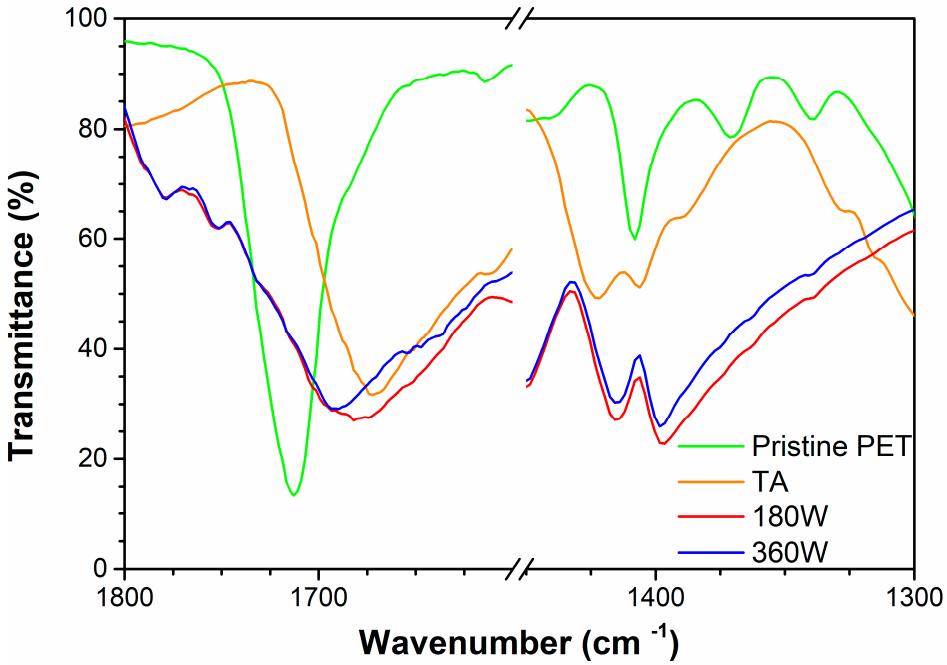

Figure 9. ATR−FTIR spectra in the range of 1300–1450 cm^{-1} and 1600–1800 cm^{-1} of pure solid terephthalic acid, pristine PET, and of the powders recovered after acidification of the microwave-treated supernatant DES/PET solution. Light green: Pristine PET, orange: Terephthalic acid, red: powder from 180 W supernatant, blue: powder from 360 W supernatant.

Table 3. FTIR peak assignment of pristine PET, TA, powder recovered from 180 W and 360 W supernatant in the regions shown in Figure 9.

Observed Signal (cm^{-1})	Assignment
1712 vs	PET C=O carbonyl stretching (ester)
1692 s	180W C=O carbonyl stretching
1678 s	360W C=O carbonyl stretching
1671 s	TA C=O carbonyl stretching (acid)
1423 s	TA C=C ring stretching + C=C-C ring stretching
1415 s	180W C=C ring stretching + C=C-C ring stretching
1415 s	360W C=C ring stretching + C=C-C ring stretching
1408 m	PET C=C ring stretching + =C-H ring in plane bending
1405 m	TA C=C ring stretching + C=C-C ring stretching
1397 s	180 W C=C ring stretching + C=C-C ring stretching
1397 s	360 W C=C ring stretching + C=C-C ring stretching
1370	PET CH_2 wagging
1340	PET CH_2 wagging

3.6. Hypothesis of Reaction Mechanism

As possible reaction mechanism for the observed depolymerization by $ZnCl_2$-urea DES, assisted by microwave radiation, we could envisage a process in which both the Lewis acidity of the electrophile (Zn^{2+}) and the Lewis basicity of urea come into play and act synergically, as recently suggested by Conroy and Zhang [70] and Wang et al. [25].

The former interaction would imply the coordination of the cation with terephthalate carbonyl oxygen, which induces a partial positive charge on it, thus rendering it highly electronegative and prone to nucleophilic attack. In the latter process, water molecules, which are always present in the DES mixture as impurities, would be "activated" by the interaction between a hydrogen atom and urea nitrogen lone pair, thus enhancing the nucleophilicity of oxygen and promoting the attack to the carbonyl group. Urea nucleophilic nitrogen could be itself involved in an additional interaction with the activated carboxyl group. (see Figure 10).

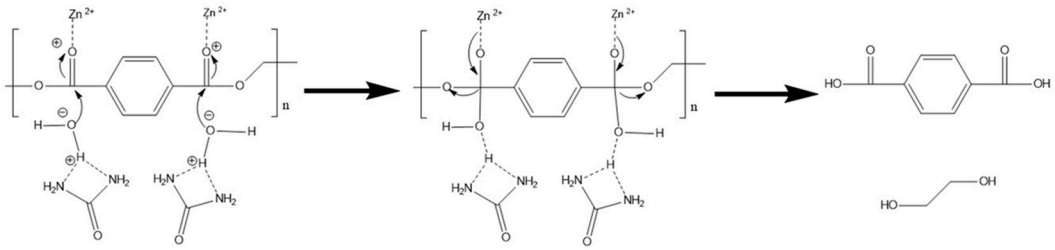

Figure 10. Proposed reaction mechanism for PET dissolution in ZnUD.

4. Conclusions

In the present study, we investigated the treatment of PET bottle shards with the type-IV Lewis Acid DES ($ZnCl_2$:urea 1:3.5) under microwave irradiation at different powers and reaction times. It was found that the treatments at 180 and 360 W resulted in a sizable weight loss of the pristine PET polymer, ranging from 8 to 10%, which changed state from a transparent polymer into an opaque white solid, while the solvent turned into a vitreous mass. The XRD and ATR–FTIR analyses of the recovered plastic fragments show that the MW treatment at low power increases the polymer crystallinity, while at higher power negligible variations are observed. After DES treatment, the solution of PET in DES

was investigated by proton NMR spectroscopy and the appearance of the peak around 7.5 ppm confirmed that TA was produced during the treatment. The infrared analysis of the recovered powders obtained after the acidic treatment of the DES-derived glass further unveils that they contain a non-negligible quantity of the acid, as testified by the appearance of the typical absorption bands of this molecule that can be observed at 1406 and 1435 cm^{-1} and below 1700 cm^{-1}. Stimulated by this promising result, we are currently investigating further combinations of DES and microwave/thermal protocols, capable of an even faster and more quantitative conversion of PET waste.

Author Contributions: Conceptualization, L.G. and C.R.; methodology, C.R.; software, L.G.; validation, M.C., C.R., and L.C.; formal analysis, M.C.; investigation, E.M.B., C.R., G.C., and L.C.; resources, M.C.; data curation, C.R. and E.M.B.; writing—original draft preparation, L.G and C.R.; writing—review and editing, L.G., C.R., and M.C.; visualization, A.L.; supervision, M.C.; project administration, M.C.; funding acquisition, M.C. All authors have read and agreed to the published version of the manuscript.

Funding: This research received no external funding.

Data Availability Statement: The original contributions presented in the study are included in the article, further inquiries can be directed to the corresponding author.

Acknowledgments: The authors thank Matteo Bonomo for the very fruitful discussions.

Conflicts of Interest: The authors declare no conflicts of interest.

References

1. Chen, L.; Pelton, R.E.O.; Smith, T.M. Comparative Life Cycle Assessment of Fossil and Bio-Based Polyethylene Terephthalate (PET) Bottles. *J. Clean. Prod.* **2016**, *137*, 667–676. [CrossRef]
2. Arena, U.; Mastellone, M.L.; Perugini, F. Life Cycle Assessment of a Plastic Packaging Recycling System. *Int. J. Life Cycle Assess.* **2003**, *8*, 92. [CrossRef]
3. Gomes, T.S.; Visconte, L.L.Y.; Pacheco, E.B.A.V. Life Cycle Assessment of Polyethylene Terephthalate Packaging: An Overview. *J. Polym. Environ.* **2019**, *27*, 533–548. [CrossRef]
4. Qualities of Common Plastic Bottle Materials. Available online: https://www.usplastic.com/knowledgebase/article.aspx?contentkey=1001 (accessed on 9 April 2024).
5. Comprehensive Guide on Polyethylene (PE). Available online: https://omnexus.specialchem.com/selection-guide/polyethylene-plastic#tubing (accessed on 9 April 2024).
6. Garcia, J.M.; Robertson, M.L. The Future of Plastics Recycling. *Science* **2017**, *358*, 870–872. [CrossRef]
7. Alzlzly, K.R.H. Recycling and Its Role in Reducing Costs and Achieving Sustainability. In *AIP Conference Proceedings*; AIP Publishing: Melville, NY, USA, 2023; p. 100001.
8. Zichittella, G.; Ebrahim, A.M.; Zhu, J.; Brenner, A.E.; Drake, G.; Beckham, G.T.; Bare, S.R.; Rorrer, J.E.; Román-Leshkov, Y. RETRACTED: Hydrogenolysis of Polyethylene and Polypropylene into Propane over Cobalt-Based Catalysts. *JACS Au* **2022**, *2*, 2259–2268. [CrossRef]
9. King, S. Recycling Our Way to Sustainability. *Nature* **2022**, *611*, S7. [CrossRef]
10. PET Market In Europe: State Of Play 2022. Available online: https://eunomia.eco/reports/pet-market-in-europe-state-of-play-2022/ (accessed on 17 April 2024).
11. Directive (EU) 2019/904 of the European Parliament and of the Council of 5 June 2019 on the Reduction of the Impact of Certain Plastic Products on the Environment (Text with EEA Relevance). Official Journal of the European Union. Available online: https://eur-lex.europa.eu/eli/dir/2019/904/oj (accessed on 17 April 2024).
12. Brivio, L.; Tollini, F. PET Recycling: Review of the Current Available Technologies and Industrial Perspectives. *Adv. Chem. Eng.* **2022**, *60*, 215–267.
13. Schyns, Z.O.G.; Shaver, M.P. Mechanical Recycling of Packaging Plastics: A Review. *Macromol. Rapid Commun.* **2021**, *42*, 2000415. [CrossRef]
14. Ragaert, K.; Delva, L.; Van Geem, K. Mechanical and Chemical Recycling of Solid Plastic Waste. *Waste Manag.* **2017**, *69*, 24–58. [CrossRef]
15. Al-Sabagh, A.M.; Yehia, F.Z.; Eshaq, G.; Rabie, A.M.; ElMetwally, A.E. Greener Routes for Recycling of Polyethylene Terephthalate. *Egypt. J. Pet.* **2016**, *25*, 53–64. [CrossRef]
16. Jeswani, H.; Krüger, C.; Russ, M.; Horlacher, M.; Antony, F.; Hann, S.; Azapagic, A. Life Cycle Environmental Impacts of Chemical Recycling via Pyrolysis of Mixed Plastic Waste in Comparison with Mechanical Recycling and Energy Recovery. *Sci. Total Environ.* **2021**, *769*, 144483. [CrossRef]

17. Ragaert, K.; Huysveld, S.; Vyncke, G.; Hubo, S.; Veelaert, L.; Dewulf, J.; Du Bois, E. Design from Recycling: A Complex Mixed Plastic Waste Case Study. *Resour. Conserv. Recycl.* **2020**, *155*, 104646. [CrossRef]
18. Tomás, R.A.F.; Bordado, J.C.M.; Gomes, J.F.P. *P*-Xylene Oxidation to Terephthalic Acid: A Literature Review Oriented toward Process Optimization and Development. *Chem. Rev.* **2013**, *113*, 7421–7469. [CrossRef]
19. Damayanti; Wu, H.-S. Strategic Possibility Routes of Recycled PET. *Polymers* **2021**, *13*, 1475. [CrossRef]
20. Barnard, E.; Rubio Arias, J.J.; Thielemans, W. Chemolytic Depolymerisation of PET: A Review. *Green. Chem.* **2021**, *23*, 3765–3789. [CrossRef]
21. George, N.; Kurian, T. Recent Developments in the Chemical Recycling of Postconsumer Poly(Ethylene Terephthalate) Waste. *Ind. Eng. Chem. Res.* **2014**, *53*, 14185–14198. [CrossRef]
22. Paparella, A.N.; Perrone, S.; Salomone, A.; Messa, F.; Cicco, L.; Capriati, V.; Perna, F.M.; Vitale, P. Use of Deep Eutectic Solvents in Plastic Depolymerization. *Catalysts* **2023**, *13*, 1035. [CrossRef]
23. Yue, Q.F.; Wang, C.X.; Zhang, L.N.; Ni, Y.; Jin, Y.X. Glycolysis of Poly(Ethylene Terephthalate) (PET) Using Basic Ionic Liquids as Catalysts. *Polym. Degrad. Stab.* **2011**, *96*, 399–403. [CrossRef]
24. Wang, Q.; Geng, Y.; Lu, X.; Zhang, S. First-Row Transition Metal-Containing Ionic Liquids as Highly Active Catalysts for the Glycolysis of Poly(Ethylene Terephthalate) (PET). *ACS Sustain. Chem. Eng.* **2015**, *3*, 340–348. [CrossRef]
25. Wang, Y.; Zhang, Y.; Song, H.; Wang, Y.; Deng, T.; Hou, X. Zinc-Catalyzed Ester Bond Cleavage: Chemical Degradation of Polyethylene Terephthalate. *J. Clean. Prod.* **2019**, *208*, 1469–1475. [CrossRef]
26. Al-Sabagh, A.M.; Yehia, F.Z.; Eissa, A.-M.M.F.; Moustafa, M.E.; Eshaq, G.; Rabie, A.-R.M.; ElMetwally, A.E. Glycolysis of Poly(Ethylene Terephthalate) Catalyzed by the Lewis Base Ionic Liquid [Bmim][OAc]. *Ind. Eng. Chem. Res.* **2014**, *53*, 18443–18451. [CrossRef]
27. Zhu, M.; Li, Z.; Wang, Q.; Zhou, X.; Lu, X. Characterization of Solid Acid Catalysts and Their Reactivity in the Glycolysis of Poly(Ethylene Terephthalate). *Ind. Eng. Chem. Res.* **2012**, *51*, 11659–11666. [CrossRef]
28. Geng, Y.; Dong, T.; Fang, P.; Zhou, Q.; Lu, X.; Zhang, S. Fast and Effective Glycolysis of Poly(Ethylene Terephthalate) Catalyzed by Polyoxometalate. *Polym. Degrad. Stab.* **2015**, *117*, 30–36. [CrossRef]
29. Fang, P.; Liu, B.; Xu, J.; Zhou, Q.; Zhang, S.; Ma, J.; lu, X. High-Efficiency Glycolysis of Poly(Ethylene Terephthalate) by Sandwich-Structure Polyoxometalate Catalyst with Two Active Sites. *Polym. Degrad. Stab.* **2018**, *156*, 22–31. [CrossRef]
30. Imran, M.; Kim, B.-K.; Han, M.; Cho, B.G.; Kim, D.H. Sub- and Supercritical Glycolysis of Polyethylene Terephthalate (PET) into the Monomer Bis(2-Hydroxyethyl) Terephthalate (BHET). *Polym. Degrad. Stab.* **2010**, *95*, 1686–1693. [CrossRef]
31. Leng, Z.; Padhan, R.K.; Sreeram, A. Production of a Sustainable Paving Material through Chemical Recycling of Waste PET into Crumb Rubber Modified Asphalt. *J. Clean. Prod.* **2018**, *180*, 682–688. [CrossRef]
32. Yang, Y.; Lu, Y.; Xiang, H.; Xu, Y.; Li, Y. Study on Methanolytic Depolymerization of PET with Supercritical Methanol for Chemical Recycling. *Polym. Degrad. Stab.* **2002**, *75*, 185–191. [CrossRef]
33. Nunes, C.S.; da Silva, M.J.V.; da Silva, D.C.; Freitas, A.D.R.; Rosa, F.A.; Rubira, A.F.; Muniz, E.C. PET Depolymerisation in Supercritical Ethanol Catalysed by [Bmim][BF_4]. *RSC Adv.* **2014**, *4*, 20308–20316. [CrossRef]
34. Leng, Z.; Sreeram, A.; Padhan, R.K.; Tan, Z. Value-Added Application of Waste PET Based Additives in Bituminous Mixtures Containing High Percentage of Reclaimed Asphalt Pavement (RAP). *J. Clean. Prod.* **2018**, *196*, 615–625. [CrossRef]
35. Tawfik, M.E.; Eskander, S.B. Chemical Recycling of Poly(Ethylene Terephthalate) Waste Using Ethanolamine. Sorting of the End Products. *Polym. Degrad. Stab.* **2010**, *95*, 187–194. [CrossRef]
36. Fukushima, K.; Coulembier, O.; Lecuyer, J.M.; Almegren, H.A.; Alabdulrahman, A.M.; Alsewailem, F.D.; Mcneil, M.A.; Dubois, P.; Waymouth, R.M.; Horn, H.W.; et al. Organocatalytic Depolymerization of Poly(Ethylene Terephthalate). *J. Polym. Sci. A Polym. Chem.* **2011**, *49*, 1273–1281. [CrossRef]
37. Liu, Y.; Wang, M.; Pan, Z. Catalytic Depolymerization of Polyethylene Terephthalate in Hot Compressed Water. *J. Supercrit. Fluids* **2012**, *62*, 226–231. [CrossRef]
38. Segura Zarate, A.Y.; Gontrani, L.; Galliano, S.; Bauer, E.M.; Donia, D.T.; Barolo, C.; Bonomo, M.; Carbone, M. Green Zinc/Galactomannan-Based Hydrogels Push up the Photovoltage of Quasi Solid Aqueous Dye Sensitized Solar Cells. *Sol. Energy* **2024**, *272*, 112460. [CrossRef]
39. Carbone, M.; De Rossi, S.; Donia, D.T.; Di Marco, G.; Gustavino, B.; Roselli, L.; Tagliatesta, P.; Canini, A.; Gismondi, A. Biostimulants Promoting Growth of *Vicia Faba* L. Seedlings: Inulin Coated ZnO Nanoparticles. *Chem. Biol. Technol. Agric.* **2023**, *10*, 134. [CrossRef]
40. Casaletto, M.P.; Carbone, M.; Piancastelli, M.N.; Horn, K.; Weiss, K.; Zanoni, R. A High Resolution Photoemission Study of Phenol Adsorption on Si(100)2 × 1. *Surf. Sci.* **2005**, *582*, 42–48. [CrossRef]
41. Kim, J.W.; Carbone, M.; Tallarida, M.; Dil, J.H.; Horn, K.; Casaletto, M.P.; Flammini, R.; Piancastelli, M.N. Adsorption of 2,3-Butanediol on Si(1 0 0). *Surf. Sci.* **2004**, *559*, 179–185. [CrossRef]
42. Caminiti, R.; Carbone, M.; Panero, S.; Sadun, C. Conductivity and Structure of Poly(Ethylene Glycol) Complexes Using Energy Dispersive X-ray Diffraction. *J. Phys. Chem. B* **1999**, *103*, 10348–10355. [CrossRef]
43. Carbone, M.; Piancastelli, M.N.; Casaletto, M.P.; Zanoni, R.; Besnard-Ramage, M.J.; Comtet, G.; Dujardin, G.; Hellner, L. Phenol Adsorption on Si(111)7 × 7 Studied by Synchrotron Radiation Photoemission and Photodesorption. *Surf. Sci.* **1999**, *419*, 114–119. [CrossRef]

44. Carbone, M.; Piancastelli, M.N.; Paggel, J.J.; Weindel, C.; Horn, K. A High-Resolution Photoemission Study of Ethanol Adsorption on Si(111)-(7 × 7). *Surf. Sci.* **1998**, *412–413*, 441–446. [CrossRef]
45. Carbone, M.; Zanoni, R.; Piancastelli, M.N.; Comtet, G.; Dujardin, G.; Hellner, L. Synchrotron Radiation Photoemission and Photostimulated Desorption of Deuterated Methanol on Si(111)7 × 7 and Si(100)2 × 1. *Surf. Sci.* **1996**, *352–354*, 391–395. [CrossRef]
46. Carbone, M.; Briancesco, R.; Bonadonna, L. Antimicrobial Power of Cu/Zn Mixed Oxide Nanoparticles to Escherichia Coli. *Environ. Nanotechnol. Monit. Manag.* **2017**, *7*, 97–102. [CrossRef]
47. Babazadeh, S.; Bisauriya, R.; Carbone, M.; Roselli, L.; Cecchetti, D.; Bauer, E.M.; Sennato, S.; Prosposito, P.; Pizzoferrato, R. Colorimetric Detection of Chromium(VI) Ions in Water Using Unfolded-Fullerene Carbon Nanoparticles. *Sensors* **2021**, *21*, 6353. [CrossRef]
48. Yoshida, S.; Hiraga, K.; Takehana, T.; Taniguchi, I.; Yamaji, H.; Maeda, Y.; Toyohara, K.; Miyamoto, K.; Kimura, Y.; Oda, K. A Bacterium That Degrades and Assimilates Poly(Ethylene Terephthalate). *Science* **2016**, *351*, 1196–1199. [CrossRef]
49. Zhong-Johnson, E.Z.L.; Voigt, C.A.; Sinskey, A.J. An Absorbance Method for Analysis of Enzymatic Degradation Kinetics of Poly(Ethylene Terephthalate) Films. *Sci. Rep.* **2021**, *11*, 928. [CrossRef]
50. Nabgan, B.; Tahir, M.; Abdullah, T.A.T.; Nabgan, W.; Gambo, Y.; Mat, R.; Saeh, I. Ni/Pd-Promoted Al_2O_3 –La_2O_3 Catalyst for Hydrogen Production from Polyethylene Terephthalate Waste via Steam Reforming. *Int. J. Hydrog. Energy* **2017**, *42*, 10708–10721. [CrossRef]
51. Campetella, M.; Montagna, M.; Gontrani, L.; Scarpellini, E.; Bodo, E. Unexpected Proton Mobility in the Bulk Phase of Cholinium-Based Ionic Liquids: New Insights from Theoretical Calculations. *Phys. Chem. Chem. Phys.* **2017**, *19*, 11869–11880. [CrossRef]
52. Sun, J.; Liu, D.; Young, R.P.; Cruz, A.G.; Isern, N.G.; Schuerg, T.; Cort, J.R.; Simmons, B.A.; Singh, S. Solubilization and Upgrading of High Polyethylene Terephthalate Loadings in a Low-Costing Bifunctional Ionic Liquid. *ChemSusChem* **2018**, *11*, 781–792. [CrossRef]
53. Rollo, M.; Raffi, F.; Rossi, E.; Tiecco, M.; Martinelli, E.; Ciancaleoni, G. Depolymerization of Polyethylene Terephthalate (PET) under Mild Conditions by Lewis/Brønsted Acidic Deep Eutectic Solvents. *Chem. Eng. J.* **2023**, *456*, 141092. [CrossRef]
54. Rollo, M.; Perini, M.A.G.; Sanzone, A.; Polastri, L.; Tiecco, M.; Torregrosa-Chinillach, A.; Martinelli, E.; Ciancaleoni, G. Effect of Chloride Salts and Microwaves on Polyethylene Terephthalate (PET) Hydrolysis by Iron Chloride/Acetic Acid Lewis/Brønsted Acidic Deep Eutectic Solvent. *RSC Sustain.* **2024**, *2*, 187–196. [CrossRef]
55. Azeem, M.; Fournet, M.B.; Attallah, O.A. Ultrafast 99% Polyethylene Terephthalate Depolymerization into Value Added Monomers Using Sequential Glycolysis-Hydrolysis under Microwave Irradiation. *Arab. J. Chem.* **2022**, *15*, 103903. [CrossRef]
56. Wang, Q.; Yao, X.; Geng, Y.; Zhou, Q.; Lu, X.; Zhang, S. Deep Eutectic Solvents as Highly Active Catalysts for the Fast and Mild Glycolysis of Poly(Ethylene Terephthalate)(PET). *Green Chem.* **2015**, *17*, 2473–2479. [CrossRef]
57. Qin, H.; Hu, X.; Wang, J.; Cheng, H.; Chen, L.; Qi, Z. Overview of Acidic Deep Eutectic Solvents on Synthesis, Properties and Applications. *Green Energy Environ.* **2020**, *5*, 8–21. [CrossRef]
58. Abbott, A.P.; Barron, J.C.; Ryder, K.S.; Wilson, D. Eutectic-Based Ionic Liquids with Metal-Containing Anions and Cations. *Chem. Eur. J.* **2007**, *13*, 6495–6501. [CrossRef]
59. Gontrani, L.; Donia, D.T.; Maria Bauer, E.; Tagliatesta, P.; Carbone, M. Novel Synthesis of Zinc Oxide Nanoparticles from Type IV Deep Eutectic Solvents. *Inorg. Chim. Acta* **2023**, *545*, 121268. [CrossRef]
60. Murthy, N.S.; Correale, S.T.; Minor, H. Structure of the Amorphous Phase in Crystallizable Polymers: Poly(Ethylene Terephthalate). *Macromolecules* **1991**, *24*, 1185–1189. [CrossRef]
61. Scherrer, P. Bestimmung Der Inneren Struktur Und Der Größe von Kolloidteilchen Mittels Röntgenstrahlen. In *Kolloidchemie Ein Lehrbuch*; Springer: Berlin/Heidelberg, Germany, 1912; pp. 387–409.
62. Patterson, A.L. The Scherrer Formula for X-ray Particle Size Determination. *Phys. Rev.* **1939**, *56*, 978–982. [CrossRef]
63. Guo, B.; Lopez-Lorenzo, X.; Fang, Y.; Bäckström, E.; Capezza, A.J.; Vanga, S.R.; Furó, I.; Hakkarainen, M.; Syrén, P. Fast Depolymerization of PET Bottle Mediated by Microwave Pre-Treatment and An Engineered PETase. *ChemSusChem* **2023**, *16*, e202300742. [CrossRef]
64. Wang, H.; Keum, J.K.; Hiltner, A.; Baer, E.; Freeman, B.; Rozanski, A.; Galeski, A. Confined Crystallization of Polyethylene Oxide in Nanolayer Assemblies. *Science* **2009**, *323*, 757–760. [CrossRef]
65. Hammond, O.S.; Bowron, D.T.; Edler, K.J. Liquid Structure of the Choline Chloride-Urea Deep Eutectic Solvent (Reline) from Neutron Diffraction and Atomistic Modelling. *Green. Chem.* **2016**, *18*, 2736–2744. [CrossRef]
66. Bahl, S.K.; Cornell, D.D.; Boerio, F.J.; McGraw, G.E. Interpretation of the Vibrational Spectra of Poly (Ethylene Terephthalate). *J. Polym. Sci. Polym. Lett. Ed.* **1974**, *12*, 13–19. [CrossRef]
67. Chen, Z.; Hay, J.N.; Jenkins, M.J. The Thermal Analysis of Poly(Ethylene Terephthalate) by FTIR Spectroscopy. *Thermochim. Acta* **2013**, *552*, 123–130. [CrossRef]
68. Yim, S.D.; Kim, S.J.; Baik, J.H.; Nam, I.; Mok, Y.S.; Lee, J.-H.; Cho, B.K.; Oh, S.H. Decomposition of Urea into NH_3 for the SCR Process. *Ind. Eng. Chem. Res.* **2004**, *43*, 4856–4863. [CrossRef]

69. Trejo-Carbajal, N.; Ambriz-Luna, K.I.; Herrera-González, A.M. Efficient Method and Mechanism of Depolymerization of PET under Conventional Heating and Microwave Radiation Using T-BuNH_2/Lewis Acids. *Eur. Polym. J.* **2022**, *175*, 111388. [CrossRef]
70. Conroy, S.; Zhang, X. Theoretical Insights into Chemical Recycling of Polyethylene Terephthalate (PET). *Polym. Degrad. Stab.* **2024**, *223*, 110729. [CrossRef]